



Wall Motion Quantification: P.R.

Deliverable D3.2

Project acronym: **THROMBUS**,

Project full title: A quantitative model of thrombosis in intracranial aneurysms

- Instrument type: Collaborative Project
- Project coordinator: CNRS

- Contract nr.: FP7-ICT-2009-6- 269966
- Start date: Feb 1, 2011
- Duration: 36 months

Report identification

Period from: 01/02/2011

To: 01/02/2012

Due date of report: 01/02/2012 (+45 days)

Submission date: 01/03/2012

Revision: Final

▪ **Dissemination level:**

PU = Public

X

Partners involved

Author of this report	Shima Sepehri	EPFL
Contributors involved in the reported work (from same organisation or others)	Prof. Jean-Philippe Thiran	EPFL
	Pascal Hagmann	EPFL
	Dr. Dominique Zosso	EPFL

Table of Contents

1	Executive Summary	7
2	Introduction	9
3	Methods and Results	11
3.1	Data acquisition	11
3.2	Registration	11
3.2.1	Threshold	11
3.2.2	Registration Algorithm	12
3.3	Segmentation	13
3.3.1	Active Contours Without Edges	13
3.3.2	Level Set Method	14
3.4	Distance Map	15
3.5	Motion Estimation	16
3.6	Validation methodology: 2D-3D Registration in the Fourier Domain.....	19
4	Conclusions	23
5	References.....	25

List of Figures

Figure 1 : The original volume (left) and the threshold image, showing the bones (right)	11
Figure 2 : The pre-processing registration scheme.....	12
Figure 3 : The difference before registration (left), and after the registration (right). Color scale represents Hounsfield Units (HU).	12
Figure 4 : An illustration of the Level Set Method.	14
Figure 5 : Left, a slice of interest in the CTA series and Right, the segmented aneurysm.....	15
Figure 6 : Left, the DM of the segmented aneurysm and right, the DM with the original segmented aneurysm (zero level (dark blue) of the DM).....	16
Figure 7: The motion tracking process.....	16
Figure 8 : a) An example of a segmented aneurysm b) A slice of interest with the corresponding segmentation on two volumes, which shows the accuracy of the segmentation method c) The maximum absolute motion of the wall of the segmented aneurysm d) The motion of a bulge area.	18
Figure 9: The motion of the bulge point of Figure 8c, across the twenty phases	18
Figure 10 : The validation scheme.	19
Figure 11 : The slice to volume registration in the Fourier domain.....	20
Figure 12 : Lateral (left) and frontal (middle) projections of the knee joint. The right figure shows the manual and automatic detections of the movement. In the first slices there is a difference between the manual and the automatic trackings which has been reduced by a reverse processing (the other blue curve)	21

1 Executive Summary

In this deliverable, the progress of the Wall Motion Quantification is explained. The goal is to describe the status of the development and validation of a method for aneurysm wall motion tracking in 4D CTA images.

The main achievements of the research at its current state can be summarized as follows:

- A registration method for reducing the CTA reconstruction artefacts has been developed,
- 3D segmentation algorithm has been implemented,
- a first version of the 4D motion estimation algorithm has been defined and implemented,
- Results on 4 cases of different aneurysm sizes and locations have been obtained,
- A validation methodology has been defined.

Intracranial aneurysm, which is a threatening problem, is commonly treated by neuro-radiological intervention. However, considering the surgery risks, an assessment of the risk of rupture can help doctors to decide better between the above-mentioned option and other options such as careful observations. Studies show that no reliable factor or method exists to predict the rupture. On the other hand, the pulsation of the wall of aneurysms, and the evidences of the coincidence of the rupture with pulsation areas brought clinical researchers to consider the hypothesis of its relationship with the rupture. However, to examine this hypothesis a reliable tool is needed for the quantification of this barely-perceptible motion. Moreover, besides the importance of the wall motion for the prediction of the rupture, there are evidences of its relationship with the thrombosis procedure, which is the natural repair of the aneurysms and the central point of interest of the THROMBUS project. Considering the lack of accuracy, automation and the ground-truth validation in previous attempts in wall motion analysis, we are developing a methodology to answer this vital need.

Since the aneurysm wall motion is very small, first global artefact movements should be removed. Afterwards, a region-based segmentation method, with a flexible and efficient computation algorithm, has been used on the registered images for segmenting the aneurysm in each volume of a time series of CTA images. These segmented volumes were then used to detect the motion between different volumes. The whole procedure was applied on a data set of four 4D ECG-Gated CTA of patients with different size and localization of the aneurysm.

The challenge of the quantification of such a barely-perceptible motion can never be completed reliably, without a realistic validation. Therefore, we defined a validation scenario, and developed the corresponding methodology to implement it.

2 Introduction

In task 3.2 of WP3, we focus on Wall Motion Tracking in Intracranial Aneurysms by means of accurate and robust segmentation in a 4D Electrocardiography (ECG)-gated Computed Tomography (CT) image series. Motion quantification of the wall of aneurysms can be a significant step in its diagnosis and treatment, not only because clinical observations show that aneurysms pulse [Meyer et al., 1993; Wardlaw and Cannon, 1996, Wardlaw et al., 1998], but also since it has been reported that the rupture sites coincide with the pulsation areas [Hayakawa et al., 2005; Ishida et al., 2005; Kato et al., 2004].

Detection of this barely-perceptible motion is a challenging task, and has been given relatively little attention in the literature. Besides the descriptive work of Hayakawa et al., 2005, Yaghmai et al., 2007, performed a quantitative analysis of the phantom only. A previous work of a group in Spain, Dempere et al., 2006 uses 2D non-rigid image registration. They also added a post processing of the recovered curve, in the Fourier Domain, in their recent work, Ouebel et al., 2007. The most relevant work of them, Zhang et al., 2009, uses a time-varying B-spline tensor field to model the pulsations, and their recent work of Ouebel et al., 2010 seems to be the implementation of the same method, on real data. The recent works of Nishida et al., 2011, and Kuroda et al., 2011, use a simple calculation of the volume, which might be considered simplistic considering the reconstruction errors. In fact, the existing state-of-the-art suffers from lack of accuracy and/or automation. Our goal is therefore to contribute to the improvement of the existing image segmentation and motion tracking models for this specific and difficult application. Since motion analysis is aimed at being used as the basis of vital decisions, its method must be validated using realistic phantoms. This is an important missing element in the recent studies, which we would also like to address.

Intracranial aneurysm is a very dangerous and widespread problem. Fortunately, by the increasing use of medical imaging in different diagnoses, un-ruptured aneurysms are nowadays detected fortuitously while checking for other problems and may be treated in one of three ways: preventive surgery, neuro-radiological intervention or careful observation. At the moment, treatment depends mainly on the size and location of the aneurysm. According to studies, and considering the risks involved in surgery, attentive observation is preferred for small aneurysms. However, a study in 2004 of 280 patients with ruptured aneurysms showed that a large proportion had small or very small aneurysms. This means that at the moment there is no reliable means of predicting the rupture. Since observations during surgery shows that the aneurysms pulse, medical researchers are keen to study further the relationship between the pulsatility and the rupture. Besides the importance of the wall motion for the prediction of the rupture, there are evidences of its relationship with the thrombosis procedure, which is the natural repair of the aneurysms [Bhatnagar et al., 1985; Kupper et al., 1989]. However, there is no existing reliable method to detect this motion.

We are therefore working on developing such a method for quantifying pulsation. This deliverable reports our progress towards this goal. The final method, results and validation will be reported by month 24 in deliverable 3.4.

Considering the fact that the motion is in the range of the noise or image artefacts, pre-processing is of utmost importance. Afterwards, we focus on improving accurate and robust segmentation. Finally, we go beyond the existing motion estimation methods, to improve current accuracy and automation.

The following sections will present the methods and results and the future perspective in the conclusion.

3 Methods and Results

3.1 Data acquisition

The data set used to test our motion tracking algorithm is a series of 4D ECG-Gated CTA images. The images are obtained through medical CT examination performed by a 64-row Multi-Slice CT-Scanner (Volume CT, General Electric, Milwaukee, Wisconsin).

This 4D ECG-Gated acquisition is selectively centred on the aneurysm and requires a supplementary 50cc contrast media injection for vascular enhancement. The reconstruction is done by the aid of a physiological signal (ECG), in order to produce images of the aneurysm at different time points over one cardiac cycle. These images are "phase-related", where their phases signify the temporal subdivision of the duration of one cardiac cycle. Thus, a same spatial image can be created at different phases of the cardiac cycle.

The helical acquisition used provides continuous coverage and therefore it is possible to generate raw data from 2 phases per cycle (50% each) up to 33 phases (3% each). Here a subdivision of cardiac cycle in 20 phases of 5% each is used.

3.2 Registration

Since 4D CTA is prone to known ring like motion artefacts, due to the lack of calibration [Zhang et. al, 2009; Feldkamp et al., 1984], we first started by registering each volume with reference to the first volume.

3.2.1 [Threshold](#)

To register the images and reduce artefact movements, we tried to register the images using bones as registration landmarks. Hence, we first applied a threshold to the volumes. Figure 1 shows an example of this thresholding step.

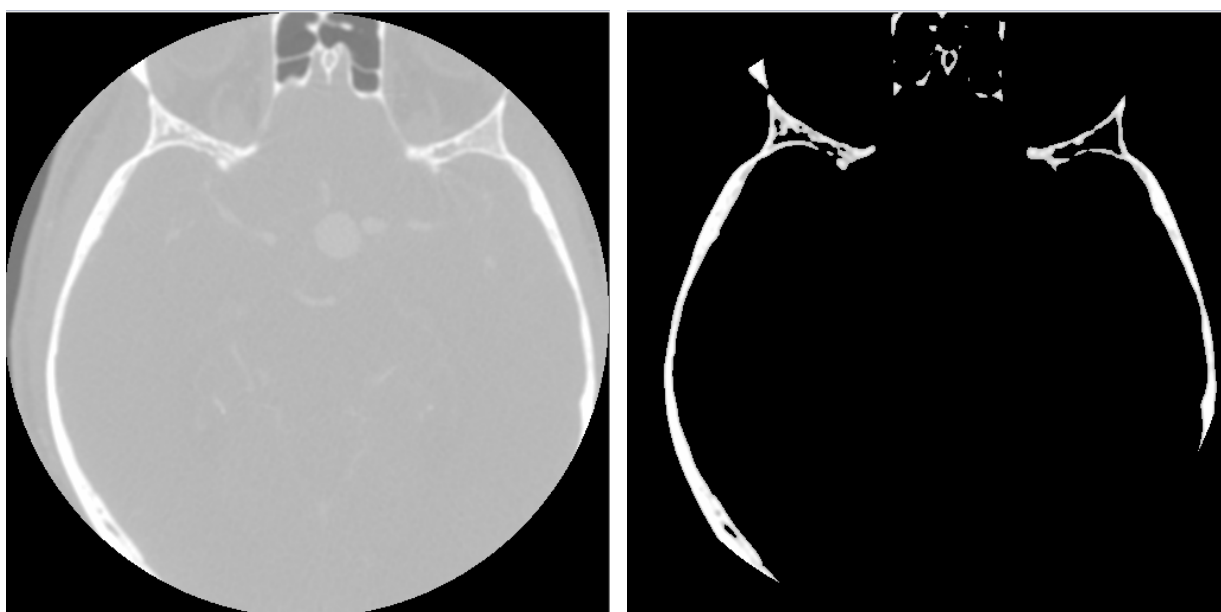


Figure 1 : The original volume (left) and the threshold image, showing the bones (right)

3.2.2 Registration Algorithm

After applying the threshold, the resulting volumes are registered, by minimizing the mean square difference between the reference and moving images, with linear interpolation and a 3D rigid transformation, as implemented in the classical ITK registration approach [Ibanez et al., 2005], as illustrated in Figure 2: after proper initialisation, an optimization scheme, in our case the classical Gradient Decent method, finds the extremum of the chosen similarity function.

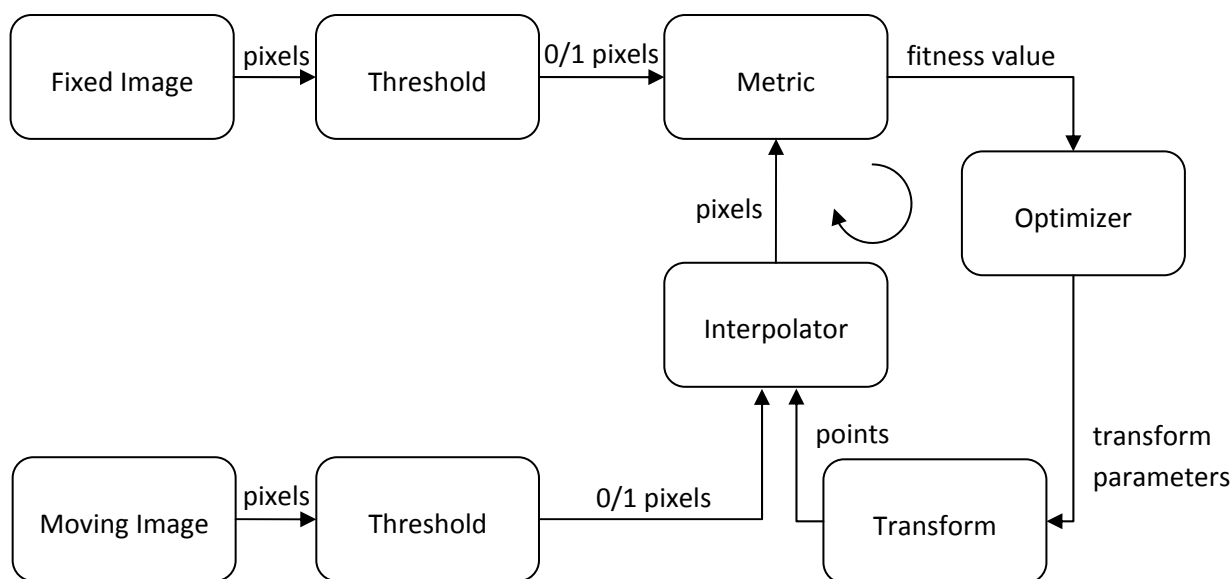


Figure 2 : The pre-processing registration scheme

The differences in the slices under observation in the two volumes, before and after the registration, are shown in Figure 3.

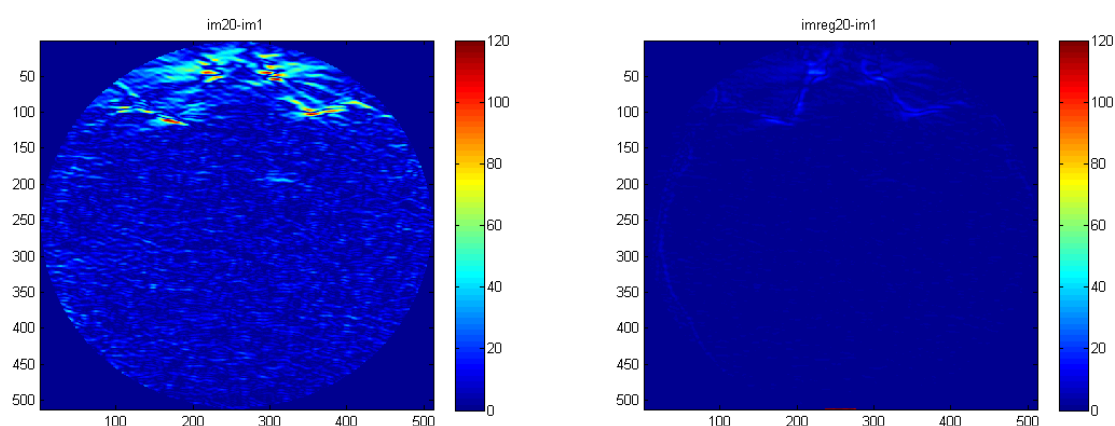


Figure 3 : The difference before registration (left), and after the registration (right). Color scale represents Hounsfield Units (HU).

3.3 Segmentation

Considering the interests of Active Contours and Level Set methods, namely their power of handling changes of topology, and adaptation to the shape of complex structures, we decided to select those methods to perform the aneurysm segmentation. Please see Deliverable 3.1 for more details on this task. We started with the 3D version of the 2 phase implementation of the Chan-Vese's Active Contours Without Edges image segmentation algorithm. The basics of this method are described below.

3.3.1 [Active Contours Without Edges](#)

Active contours are popular image segmentation models, due to their well-rooted theories and stable numerical implementations. As a reminder, image segmentation aims at determining the object contours by computing homogeneous regions and/or contours of the objects. Active contour models define energy functional with opposite terms, for example internal or regularization terms, which insure the smoothness of the curve, and an external energy that is minimal, for instance, on high values of the gradient of the image. Then, the calculus of variations is used to determine the extremum of the above-mentioned functional, which will be the object boundaries. The calculus of variations determines the extremal value (minimum/maximum) of integrals of type

$$F(u) = \int_{\Omega} f(u(x), u_x(x)) dx \quad (1)$$

The extremum of $F(u)$ is found by solving the corresponding Euler-Lagrange Equation. The success of the segmentation process depends on the suitability of the model for the application.

Here, an active contour, region-based segmentation method was used. The Chan-Vese [Chan and Vese, 2001] model revisits the Mumford-Shah model, where the energy function is defined as:

$$F_{MS}(I, C) = \int_{\Omega} |I - I_0|^2 dx + \mu \int_{\Omega \setminus C} |\nabla I|^2 dx + \nu \text{Length}(C) \quad (2)$$

I is the piecewise smooth approximation of the original image I_0 and C represents the discontinuity set representing the edges. We see that this function can be written as the integral in (1), and hence its optimal value is found by solving the Euler-Lagrange Equation.

In the Chan-Vese model, the following two assumptions are added to equation 2.

- The image has only 2 regions.
- The intensity is constant inside each region, therefore $\nabla I = 0$ except on the contours.

So, the Chan-Vese *Active Contours Without Edges* can be formulated as follows:

$$F_{ACWE}(C) = \int_C ds + \lambda \int_{c_{in}} (I - \mu_{in})^2 dx + \int_{c_{out}} (I - \mu_{out})^2 dx \quad (3)$$

where μ_{in} , μ_{out} are the mean intensity inside and outside the object.

3.3.2 [Level Set Method](#)

The Level Set Method [Osher and Sethian, 1988] is a powerful numerical scheme for modelling time-varying techniques. This method can be best illustrated in Figure 4. It shows that in this method, 2D curves are considered as the zero-level of a 3D function. As the figure demonstrates, this permits to define the difficult transformation between the curves as an easy up/down movement of the zero-level.

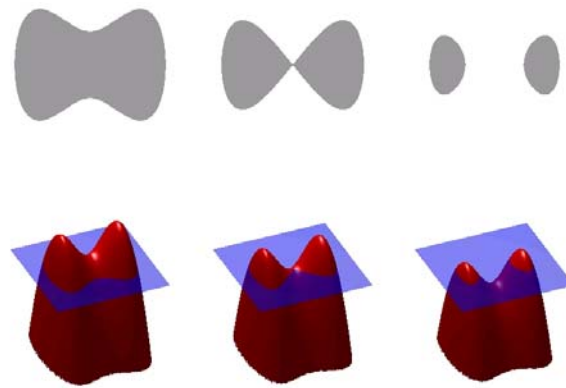


Figure 4 : An illustration of the Level Set Method.

If we define the contour as the zero level of a function ϕ , and substitute the unknown C with ϕ , we can rewrite the function in (3), in terms of Heaviside functions. Afterwards Chan and Vese use a regularization form for the Heaviside and found the Euler Lagrange Equation for ϕ as

$$\frac{\partial \Phi}{\partial t} = \delta_\epsilon \left[\operatorname{div} \left(\frac{\nabla \Phi}{|\nabla \Phi|} \right) - v - \lambda_1 (u_0 - c_1)^2 + \lambda_2 (u_0 - c_2)^2 \right] = 0 \text{ in } (0, \infty) \times \Omega, \quad (4)$$

$$\Phi(0, x, y) = \Phi_0(x, y) \text{ in } \Omega,$$

$$\frac{\delta_\epsilon(\phi)}{|\nabla \Phi|} \frac{\partial \phi}{\partial \vec{n}} = 0 \text{ on } \partial \Omega$$

Where \vec{n} denotes the exterior normal to the boundary $\partial \Omega$, and $\frac{\partial \phi}{\partial \vec{n}}$ denotes the normal derivative of ϕ at the boundary.

After numerical approximation, this model and method was implemented. Figure 5 shows an example of the resulting segmented aneurysm.

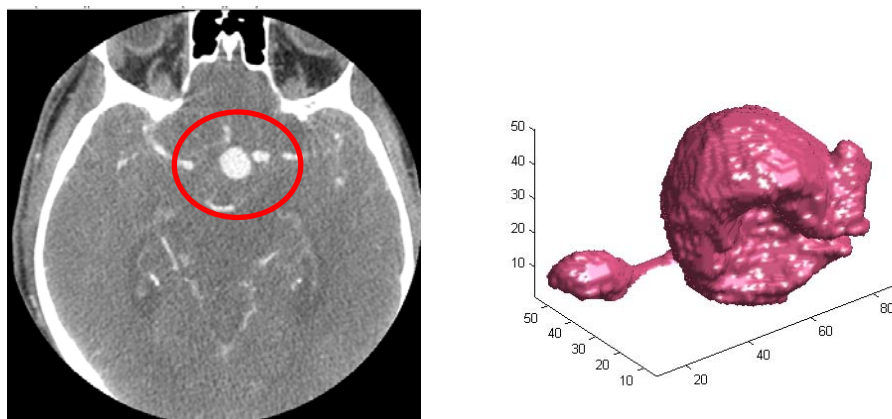


Figure 5 : Left, a slice of interest in the CTA series and Right, the segmented aneurysm.

Notice that this segmentation method will be compared with others developed by CREATIS in this project, and presented in Deliverable 3.1.

3.4 Distance Map

After segmentation, the next step towards wall motion estimation is the calculation of the distance map for each segmented volume. At a given point x of the image grid, the motion of the front is described by the Eikonal equation

$$\|\nabla T(x)\| \cdot F(x) = 1$$

where T is the arrival time of the front at x and F is the speed of the front (usually $F = 1$).

If the 3D contour is considered as a front, its distance map can be calculated using the Fast Marching Method (FMM). To perform this method, we first select a set of starting points and tag them as known. The pixels positioned one pixel from those already known are the narrow band, tagged as trial points, and the rest are far pixels. The idea is to move forward the front, freezing the values of the known points, and bring new points to the narrow band. The process therefore can be described as the following iterative scheme:

- The distance (arrival time) is calculated for all trial points, by solving the Eikonal equation.
- The trial point with the smallest arrival time is chosen and tagged as known.
- All the six-connected neighbours of this trial point are tagged as trial.
- The procedure is repeated until full calculation or until the stopping criterion has been reached

Figure 6 shows the 3D distance map (DM), using the FMM, for the segmented volume of Figure 5.

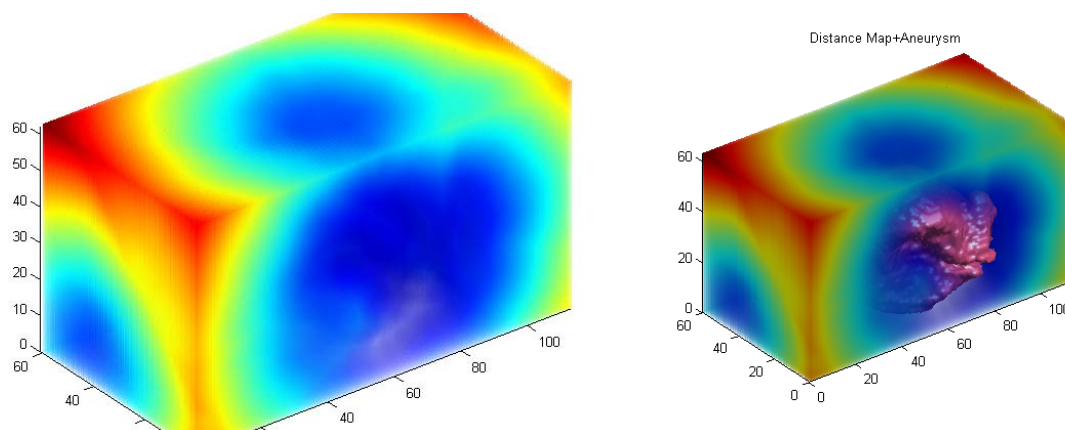


Figure 6 : Left, the DM of the segmented aneurysm and right, the DM with the original segmented aneurysm (zero level (dark blue) of the DM).

3.5 Motion Estimation

Finally, the motion tracking is achieved by evaluating the distance map of a volume of reference over the contours of a chosen volume. This is illustrated in Figure 7.

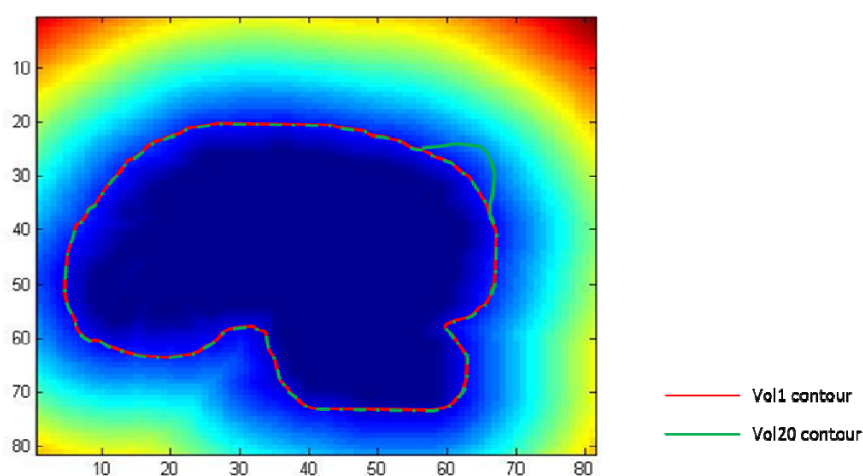
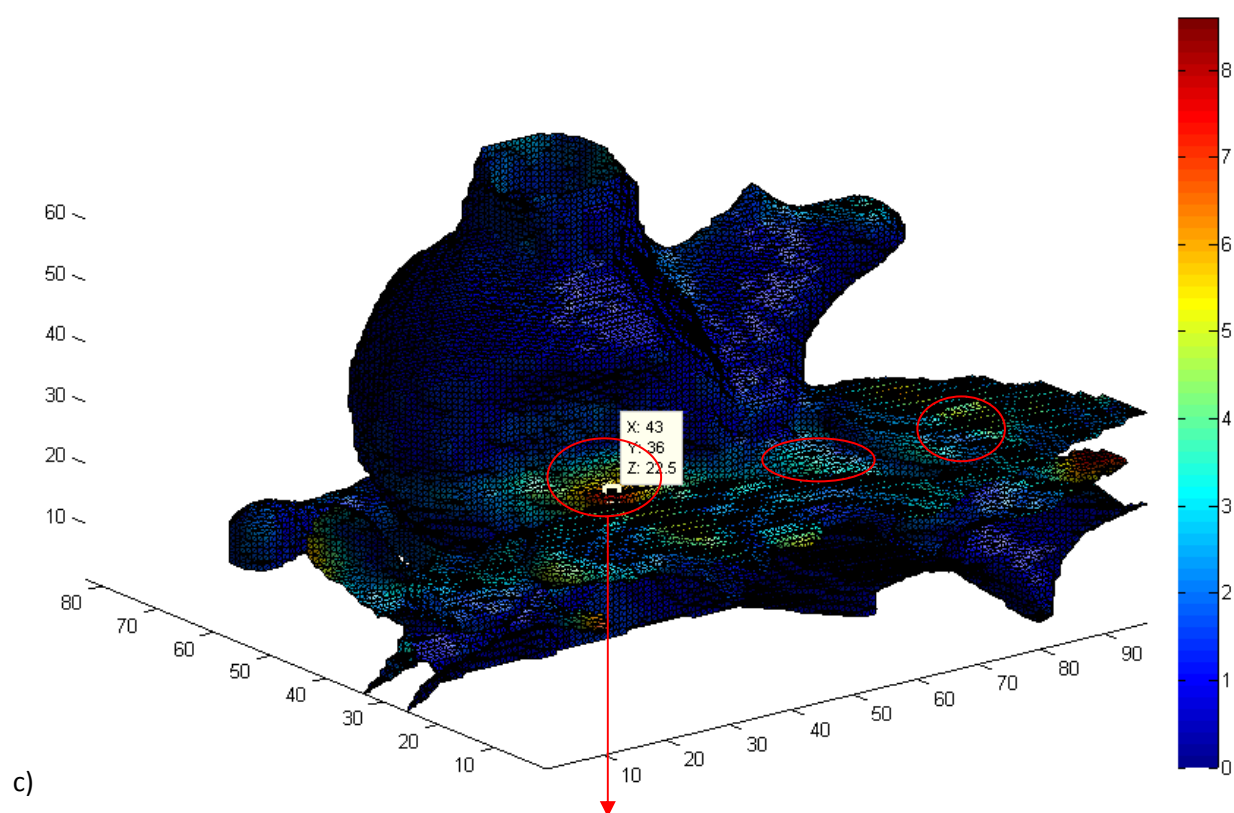
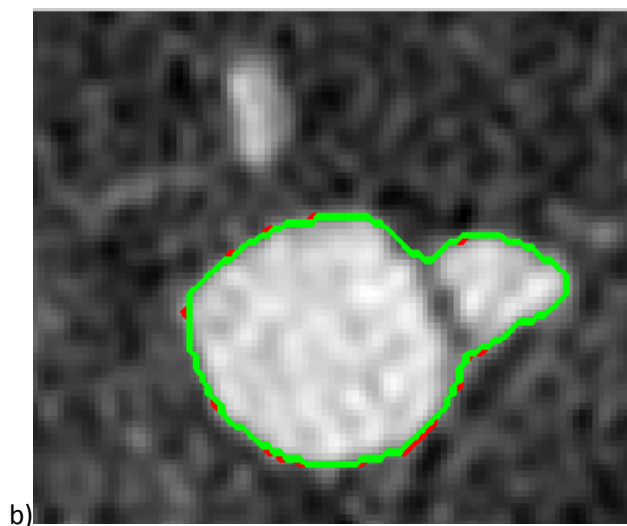
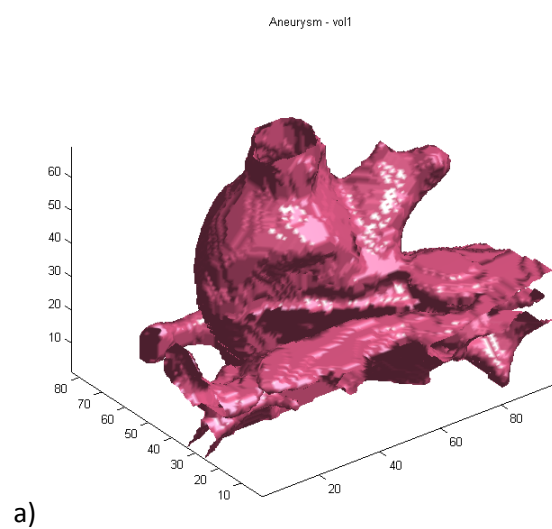


Figure 7: The motion tracking process.

In our example, consider that the contour of the aneurysm in volume 20 is deformed from volume 1, as shown above. The further the green contour, the bigger the value of the distance map of volume 1 will be at that point. This is why the evaluation of the distance map on the contours will give the motion estimation.

Figure 8 shows the maximum absolute value motion of each point of the volume during the 20-phase cardiac cycle, with the first volume as the reference. The colour index shows the motion in voxels, without rescaling. As expected, a small motion is detected on the bulges. The motion of a bulge point through time is depicted in Figure 9.



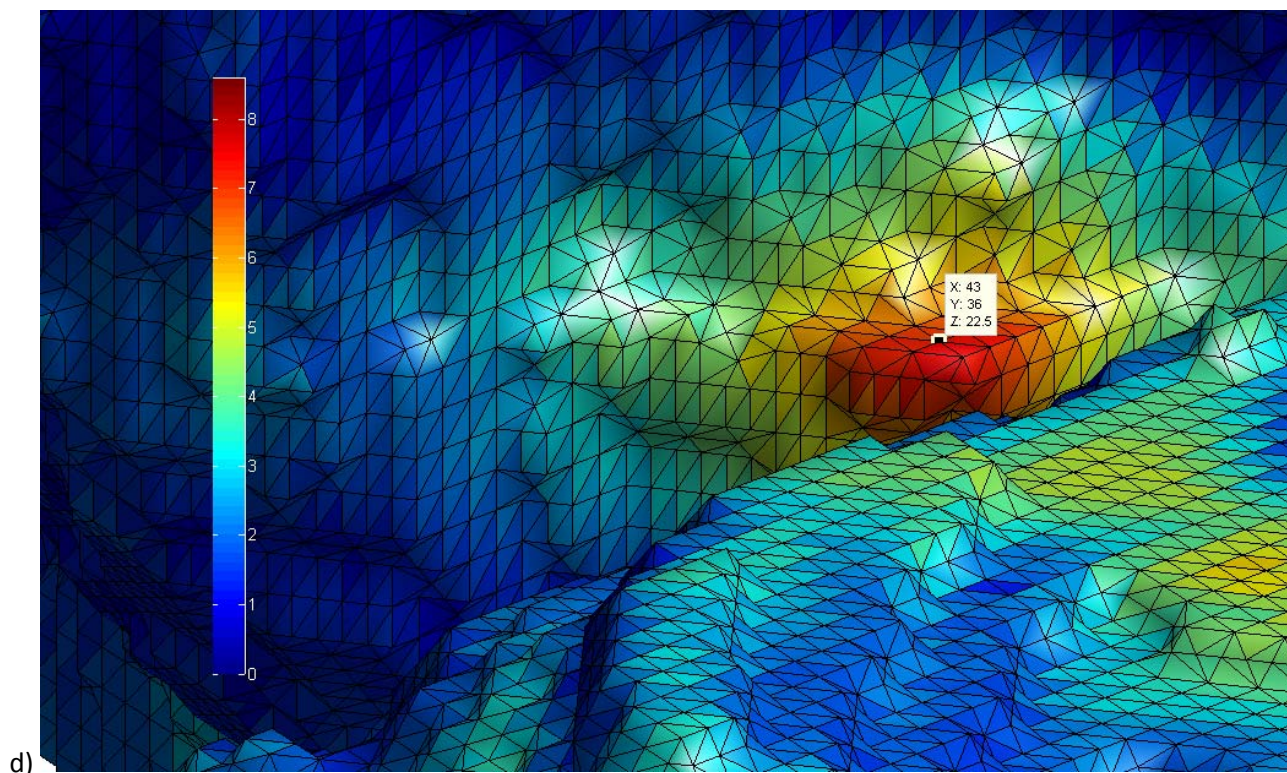


Figure 8 : a) An example of a segmented aneurysm b) A slice of interest with the corresponding segmentation on two volumes, which shows the accuracy of the segmentation method c) The maximum absolute motion of the wall of the segmented aneurysm d) The motion of a bulge area.

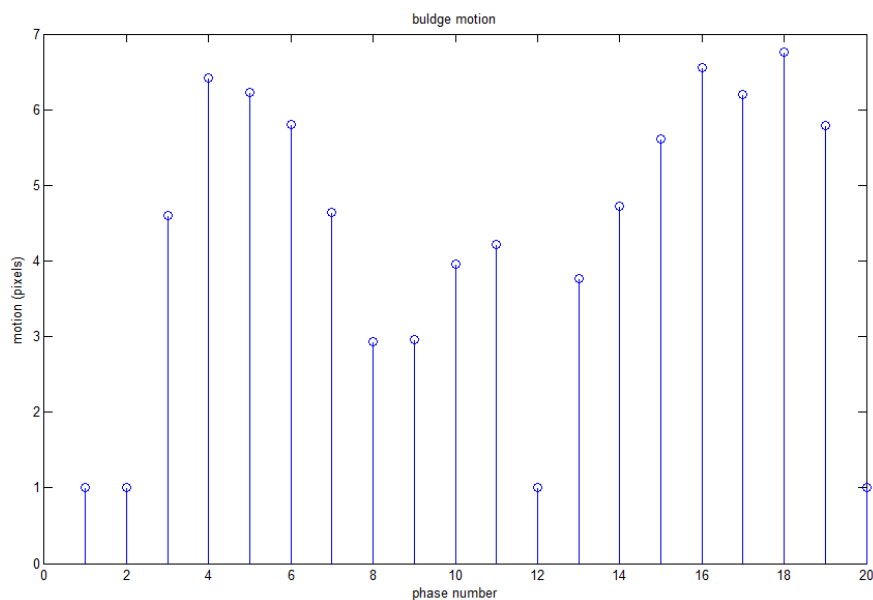


Figure 9: The motion of the bulge point of Figure 8c, across the twenty phases

Further processing, comparison, validation and clearer demonstration are still in progress.

3.6 Validation methodology: 2D-3D Registration in the Fourier Domain

As described in the previous sections, the validation of the estimated motion is of utmost importance. We have therefore spent a significant time in carefully defining a methodology that will allow in-vitro and in-vivo validation of the wall motion estimation. This validation will be conducted during the two remaining years of the project.

The in-vitro validation will involve a complete experimental setup defined by our colleagues at ULB, partners of the THROMBUS project. This setup involved a complete blood-like fluid circulation system, including pulsate flow. Silicon synthetic aneurysm, made from real geometries of intracranial aneurysms, will be built and inserted in the setup. It will then be possible to image this aneurysm with a variety of imaging protocols, including our 4D ECG-gated CT protocol, but also with high spatial and temporal resolution techniques, including classical 2D angiograms. See Figure 10.

Similarly, the in-vivo validation will include the acquisition of our 4D CT scans as well as of 2D angiograms of the same aneurysm.

In order to validate the algorithm, we need to know the ground-truth motion value. However this is not possible in either of the above-mentioned validation. The reason is that for the in-vivo validation, we do not have any control on the real motion and even for the in-vitro validation where we can tune the source of the pulsation, we do not know the value of the motion that this source will produce.

In both cases, the high-resolution angiograms will only display a projection of the aneurysm and of its motion. Our validation will consist of assessing the similarity between the perceived motions in the 2D+t projected angiograms and in the corresponding projection of our 3D+t CT scan. Therefore, both for the in-vivo and the in-vitro validation procedures, we will need to establish the correspondence between 3D volumes and 2D projections. This problem is called Projection Volume Registration.

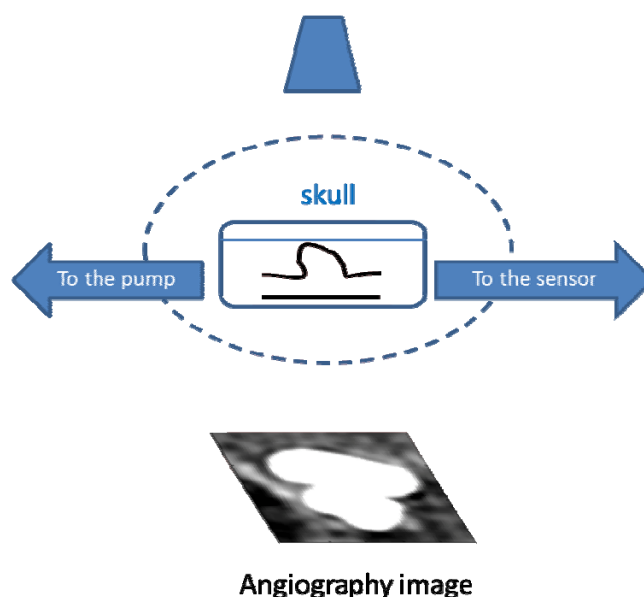


Figure 10 : The validation scheme.

The idea of Projection Volume Registration methods is to match a volume with projections. The traditional methods such as Digitally Rendered Radiography (DRR) consist of heavy computations. Therefore, we developed an alternative, faster, 2D-3D registration method in the Fourier Domain, introduced by Zosso et al., 2008. The principles of this method are as follows:

The 3D Fourier Transform of a 3D volume $f(x,y,z)$ is defined as

$$\hat{f}(\mu, \nu, \omega) = \iiint f(x, y, z) e^{-j(\mu x + \nu y + \omega z)} dx dy dz \quad (5)$$

Then, with a corollary to the central slice theorem in 3D, we can write

$$\hat{f}(\mu, \nu, 0) = \iiint f(x, y, z) e^{-j(\mu x + \nu y)} dx dy dz = \iint \left[\int f(x, y, z) dz \right] e^{-j(\mu x + \nu y)} dx dy = \hat{p}_z(\mu, \nu) \quad (6)$$

where f is the scanned volume and p is the image, according to the Radon Transform. In fact, under the parallel X-ray approximation, it can be seen that the grey level of each point (r, θ) on the rotational series is proportional to the attenuation of the X-ray during its path, and therefore proportional to the line integral of the object across its path, as in (7).

$$p_z(r, \theta) = \iint f_z(x, y) \delta(x \cos \theta + y \sin \theta - r) dx dy \quad (7)$$

Equation (6) states that the central 2D slice of the 3D Fourier volume and the 2D Fourier of the projection image are the same. This key idea facilitates the registration methods, in the sense that instead of calculating the projections from the volume and then matching these simulated projections with the original projections, we can directly match the Fourier Transform of the projections, with their corresponding slices in the Fourier Transform of the volume. This idea is illustrated in Figure 11.

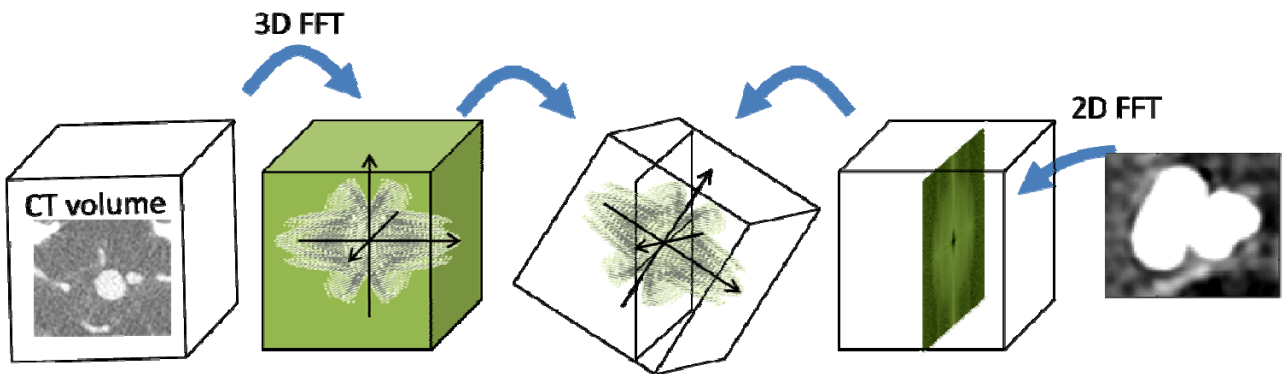


Figure 11 : The slice to volume registration in the Fourier domain.

To match the slice and the volume, it should be noticed that a rotation in the spacial domain corresponds to a rotation in the Fourier domain.

$$f_2(\omega) = f_1(R(x + \Delta x))$$

(8)

$$\begin{aligned} \hat{f}_2(\omega) &= \int \hat{f}_1(R(\mathbf{x} + \Delta \mathbf{x})) e^{-j\omega \cdot \mathbf{x}} d\mathbf{x} = e^{-j\omega \cdot \Delta \mathbf{x}} \int \hat{f}_1(R(\mathbf{x}')) e^{-j\omega \cdot \mathbf{x}'} d\mathbf{x}' \\ &= e^{-j\omega \cdot \Delta \mathbf{x}} \int \hat{f}_1(\mathbf{x}'') e^{-j(R\omega \cdot \mathbf{x}'')} d\mathbf{x}'' \end{aligned}$$

$$[\hat{f}_2(\omega)] = [\hat{f}_1(R(\omega))]$$

This method has been used to track bone movements in stereoscopic X-ray fluoroscopic image series of the knee joint [Zosso et al., 2008]. Figure 12 shows the result of the motion tracking performed with this method. The white circles show the Gaussian masks representing the region of interest. A manual tracking was also performed and compared with the algorithm results. Although the manual and automatic trackings are in good agreement, there still exist some errors, which can be partially explained by the limitation of the manual tracking and also by the assumption of parallel beam rays. As part of our effort towards the validation of our wall motion estimation algorithms, we have further developed the original method proposed by D. Zosso. We have implemented it using the ITK library and have validated it on new series of 3D volumes and 2D projection, also coming from CT and fluoroscopic images of a knee, since synthetic aneurysm volumes and angiographic projections have not been acquired so far in the project. This work is the foundation of our validation methodology which will be fully developed in the next phases of THROMBUS.

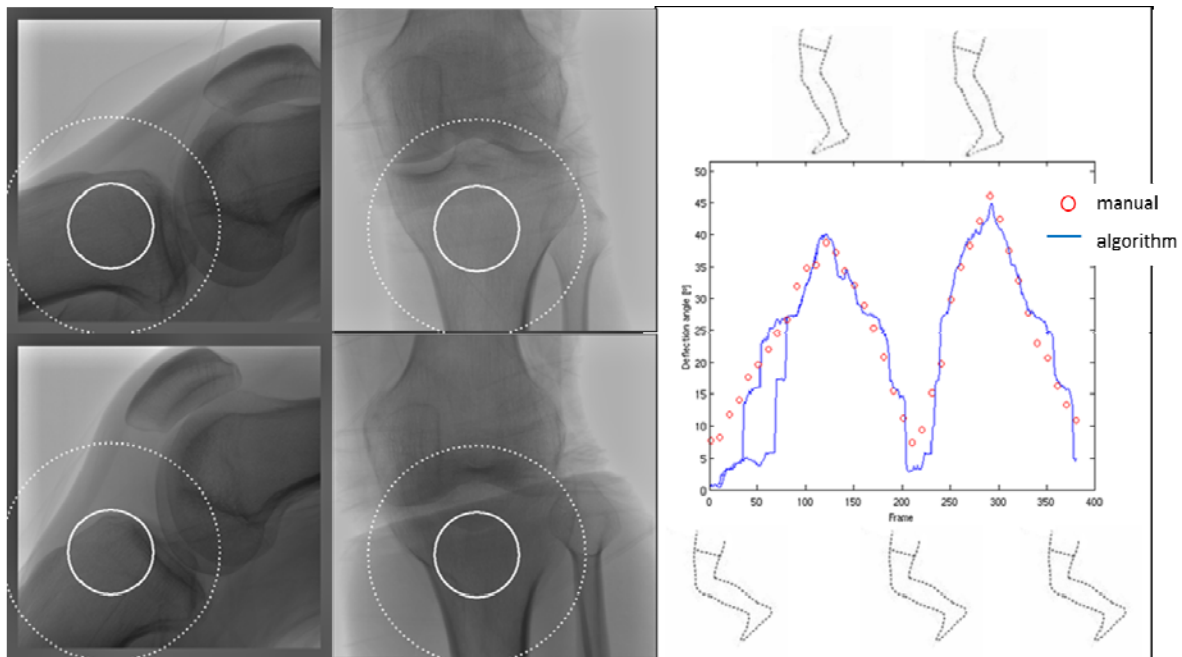


Figure 12 : Lateral (left) and frontal (middle) projections of the knee joint. The right figure shows the manual and automatic detections of the movement. In the first slices there is a difference between the manual and the automatic trackings which has been reduced by a reverse processing (the other blue curve)

4 Conclusions

During the first year, we already developed a good segmentation algorithm and motion tracking, as well as an efficient validation scheme. The results show acceptable performance; however, this should be, of course, developed in the future, especially by processing more data.

Regarding the future steps, we will first focus on the important task of validation of the algorithm, followed by fast implementation and convex formulation. Moreover, there exist different methodological improvements that we are planning to implement and compare. They include

- 4D segmentation: a good 4D smoothing criterion can avoid jerky, incorrect motion and help to keep the motion at different times in relation with the motion at other time points. On the other hand, it should be taken into account that a regularization term can increase the risk of omitting a barely-perceptible motion like that of the wall of aneurysms. These two considerations make 4D segmentation a challenge, which should be addressed, in future.
- Direct motion estimation - Optical Flow: instead of multi-segmentation, the concept of optical flow can be used in order to avoid the accumulation of errors of segmentation. In this approach a volume of reference is first segmented to find the contours of the object. In the next step, the grey level of a pixel on the contour is searched in other volumes to find the motion of that point.
- Reconstruction: considering the range of the motion we are looking for, any possible source of error can cause intolerable artefacts. Therefore, we are considering some forms of *intelligent* reconstruction particularly designed for the motion tracking. In other words, we believe that if we know what we are seeking from the data set, we can reconstruct the CT volume accordingly, paying more attention to the goal.
- Fast implementation: To deal with voluminous data and meet the required interactivity, fast implementation is a must. For this purpose, we will consider methodological improvements, such as primal-dual decomposition and the split Bregman method and also GPU implementation.

5 References

- Ares, R., 2008. Segmentation and motion analysis of aneurysms in dynamic CT images, MS thesis, EPFL, Signal Processing Lab.
- Bhatnagar, S. K., Hudak, A., Al-Yusuf, A. R., 1985. Left ventricular thrombosis, wall motion abnormalities, and blood viscosity changes after first transmural anterior myocardial infarction. *Chest*, 88 (1), 40-44.
- Bresson, X., Esedoglu, S., Vandergheynst, P., Thiran, J.P., Osher, S., 2007. Fast Global Minimization of the Active Contour/Snake Model. *J. of Math. Imag. and Vis.* 28 (2)1: 51-167.
- Chan, T., Vese, L., 2001. Active contours without edges, *IEEE Trans. Image Process.* 10 (2), 266–277.
- Feldkamp, L.A., Davis, L.C., Kress, J.W., 1984, Practical cone-beam algorithm, *J. of the Opt. Soc. of A.* 1(6): 612-619
- Goldstein T., Osher, S., 2008. The Split Bregman Algorithm for L1 Regularized Problems. *UCLA CAM Reprints* (08-29).
- Hayakawa M., Katada K., Anno H., Imizu S., Hayashi J., Irie K., Negoro M., Kato Y., Kanno T., Sano H. , 2005. CT angiography with electrocardiographically gated reconstruction for visualizing pulsation of intracranial aneurysms: identification of aneurysmal protuberance presumably associated with wall thinning. *AJNR Am J Neuroradiol.* 26(6), 1366-9.
- Ibanez, L., Schroeder, W., Ng, L., Cates, J., 2005. The ITK Software Guide. Kitware, Inc., <http://www.itk.org/ItkSoftwareGuide.pdf>, second ed.
- Ishida, F., Ogawa, H., Simizu, T., Kojima, T., Taki, W., 2005. Visualizing the dynamics of cerebral aneurysms with four-dimensional computed tomographic angiography. *Neurosurgery*, 57 (3), 460–471.
- Kato, Y., Hayakawa, M., Sano, H., Sunil, M., Imizu, S., Yoneda, M., Watanabe, S., Abe, M., Kanno, T., 2004. Prediction of impending rupture in aneurysms using 4D-CTA: Histopathological verification of a real-time minimally invasive tool in unruptured aneurysms. *Minim. Invasive Neurosurg.*, 47, pp. 131–135.
- Katsevich, A., Basu, S., Hsieh, J., 2004. Exact filtered backprojection reconstruction for dynamic pitch helical cone beam computed tomography, *Phys. Med. Biol.*, 49, 3089–3103.
- Kossioris G., Papaharilaou Y., Zohios C., 2008. Detection of Lumen, thrombus and outer wall boundaries of abdominal aortic aneurysm from 2D medical images, using level set methods, *Proceedings of the ASME 2008 Summer Bioengineering Conference (SBC2008)* June 25-29, Marriott Resort, Marco Island, Florida, USA
- Kupper, A., J., Verheugt, F., W., Peels, C., H., Galema, T., W., Roos, J., P., 1989. Left ventricular thrombus incidence and behavior studied by serial two-dimensional echocardiography in acute anterior myocardial

infarction: left ventricular wall motion, systemic embolism and oral anticoagulation. *J Am Coll Cardiol.*, 13 (7), 1514-1520

Lorigo, L.M., Faugeras, O., Grimson, W.E.L., Keriven, R., Kikinis, R., Nabavi, A., Westin, C.F., 2000. Codimension-two geodesic active contours for the segmentation of tubular structures. In: *IEEE Conference on Computer Vision and Pattern Recognition*, vol. 1, pp. 444–451.

Meyer, F., Huston III, J., Riederer, S., 1993. Pulsatile increases in aneurysm size determined by cine phase-contrast MR angiography. *J. Neurosurg.*, 78(6), pp. 879–883.

Osher, S., Sethian, J.A., 1988. Fronts propagating with curvature- dependent speed: Algorithms based on Hamilton–Jacobi formulations. *J. Comput. Phys.* 79, 12–49.

van Bemmelen, C.M., Spreeuwiers, L.J., Viergever, M.A., Niessen, W.J., 2003. Level-set-based artery-vein separation in blood pool agent CE-MR angiograms. *IEEE Trans. Med. Imaging* 22 (10), 1224– 1234.

Yaghamai, V., Rohany, M., Shaibani, A., Huber, M., Soud, H., Russell, E.J., Walker, M.T., 2007. Pulsatility imaging of saccular aneurysm model by 64-slice CT with dynamic multiscan technique, *J. Vasc. Intervent. Radiol.* 18 785–8.

Wardlaw, J., Cannon, J., 1996. Color transcranial “power” Doppler ultrasound of intracranial aneurysms. *J. Neurosurg.*, 84 (3), 459–461.

Wardlaw, J., Cannon, J., Statham, P., Price, R., 1998. Does the size of intracranial aneurysms change with intracranial pressure? Observations based on color “power” transcranial Doppler ultrasound. *J. Neurosurg.*, 88 (5), pp. 846–850, 1998.

Zhang, C., Villa-Uriol, M.C., De Craene, M., Pozo J, Frangi A., 2009. Morphodynamic Analysis of Cerebral Aneurysm Pulsation From Time-Resolved Rotational Angiography, 28 (7), 1105-1116.

Zosso, D., Bach Cuadra, M., Thiran, J.-P., 2007. Direct fourier tomographic reconstruction image-to-image filter, *Insight Journal*.

Zosso, D., Le Callennec, B., Bach Cuadra, M., Aminian, K., Jolles, B.M., Thiran, J.P., 2008. Bi-planar 2D to-3D registration in Fourier domain for stereoscopic x-ray motion tracking, in *SPIE Medical Imaging: Imaging Processing*, edited by J. M. Reinhardt and J. P. W. Pluim, SPIE Press, Bellingham, Vol. 6914, p. 69140I.